


RESEARCH

Open Access



# PSEN1-selective gamma-secretase inhibition in combination with kinase or XPO-1 inhibitors effectively targets T cell acute lymphoblastic leukemia

Inge Govaerts<sup>1,2,3</sup>, Cristina Prieto<sup>1,2,3</sup>, Charlien Vandersmissen<sup>1,2,3</sup>, Olga Gielen<sup>1,2,3</sup>, Kris Jacobs<sup>1,2,3</sup>, Sarah Provost<sup>1,2,3</sup>, David Nittner<sup>2</sup>, Johan Maertens<sup>3,4,5</sup>, Nancy Boeckx<sup>6,7</sup>, Kim De Keersmaecker<sup>3,7</sup>, Heidi Segers<sup>3,7,8</sup> and Jan Cools<sup>1,2,3\*</sup> 

## Abstract

**Background:** T cell acute lymphoblastic leukemia (T-ALL) is a high-risk subtype that comprises 10–15% of childhood and 20–25% of adult ALL cases. Over 70% of T-ALL patients harbor activating mutations in the NOTCH1 signaling pathway and are predicted to be sensitive to gamma-secretase inhibitors. We have recently demonstrated that selective inhibition of PSEN1-containing gamma-secretase complexes can overcome the dose-limiting toxicity associated with broad gamma-secretase inhibitors. In this study, we developed combination treatment strategies with the PSEN1-selective gamma-secretase inhibitor MRK-560 and other targeted agents (kinase inhibitors ruxolitinib and imatinib; XPO-1 inhibitor KPT-8602/eltanexor) for the treatment of T-ALL.

**Methods:** We treated T-ALL cell lines in vitro and T-ALL patient-derived xenograft (PDX) models in vivo with MRK-560 alone or in combination with other targeted inhibitors (ruxolitinib, imatinib or KPT-8602/eltanexor). We determined effects on proliferation of the cell lines and leukemia development and survival in the PDX models.

**Results:** All NOTCH1-signaling-dependent T-ALL cell lines were sensitive to MRK-560 and its combination with ruxolitinib or imatinib in JAK1- or ABL1-dependent cell lines synergistically inhibited leukemia proliferation. We also observed strong synergy between MRK-560 and KPT-8602 (eltanexor) in all NOTCH1-dependent T-ALL cell lines. Such synergy was also observed in vivo in a variety of T-ALL PDX models with NOTCH1 or FBXW7 mutations. Combination treatment significantly reduced leukemic infiltration in vivo and resulted in a survival benefit when compared to single treatment groups. We did not observe weight loss or goblet cell hyperplasia in single drug or combination treated mice when compared to control.

**Conclusions:** These data demonstrate that the antileukemic effect of PSEN1-selective gamma-secretase inhibition can be synergistically enhanced by the addition of other targeted inhibitors. The combination of MRK-560 with KPT-8602 is a highly effective treatment combination, which circumvents the need for the identification of additional mutations and provides a clear survival benefit in vivo. These promising preclinical data warrant further development of combination treatment strategies for T-ALL based on PSEN1-selective gamma-secretase inhibition.

\*Correspondence: jan.cools@kuleuven.be

<sup>1</sup> Center for Human Genetics, KU Leuven, Leuven, Belgium

Full list of author information is available at the end of the article



© The Author(s) 2021. **Open Access** This article is licensed under a Creative Commons Attribution 4.0 International License, which permits use, sharing, adaptation, distribution and reproduction in any medium or format, as long as you give appropriate credit to the original author(s) and the source, provide a link to the Creative Commons licence, and indicate if changes were made. The images or other third party material in this article are included in the article's Creative Commons licence, unless indicated otherwise in a credit line to the material. If material is not included in the article's Creative Commons licence and your intended use is not permitted by statutory regulation or exceeds the permitted use, you will need to obtain permission directly from the copyright holder. To view a copy of this licence, visit <http://creativecommons.org/licenses/by/4.0/>. The Creative Commons Public Domain Dedication waiver (<http://creativecommons.org/publicdomain/zero/1.0/>) applies to the data made available in this article, unless otherwise stated in a credit line to the data.

**Keywords:** Leukemia, Oncogenes, Targeted therapy, Mouse models, Gamma-secretase complex, Signaling, Nuclear export, Toxicity

## Background

Acute lymphoblastic leukemia (ALL) is an aggressive hematological malignancy characterized by a rapid clonal expansion of immature lymphocytes that infiltrate the bone marrow. T cell acute lymphoblastic leukemia (T-ALL) comprises 10–15% of childhood and 20–25% of adult cases of ALL and is considered a high-risk subtype of this aggressive hematological malignancy [1]. Despite the increase in cure rates with intensified chemotherapy treatment, the prognosis remains poor for primary refractory or relapsed ALL and the likelihood of favorable outcome steeply declines with increasing age [2].

At diagnosis, T-ALL patients carry 10–20 genomic lesions, including coding mutations and structural variants, which can increase by twofold in adults or in case of relapse [3, 4]. T-ALL is typically characterized by ectopic expression of an oncogenic transcription factor (TLX1, TLX3, TAL1, NKX3-1) and loss of cell cycle regulators CDKN2A/CDKN2B. Other aberrations typically cause activation of signaling pathways, such as NOTCH1 signaling, the JAK-STAT pathway, RAS-MAPK signaling or the PI3K-AKT-mTOR pathway. Chromosomal rearrangements can lead to expression of fusion genes, such as the NUP214-ABL1 [5] or ETV6-ABL1 fusion kinases [6]. Finally, mutations can alter the function of epigenetic regulators and chromatin remodelers or influence RNA processing [7, 8].

Through sequencing efforts in the past decade, the genomic landscape of T-ALL was revealed and provided new insight into the molecular mechanisms that drive leukemogenesis and exposed new targets for treatment [2, 7, 8]. Over 70% of T-ALL patients carry gain-of-function mutations in transmembrane receptor NOTCH1, inducing ligand-independent activation or delayed degradation of intracellular NOTCH1. Alternatively, loss-of-function mutations of ubiquitin-ligase FBXW7 also cause delayed degradation of intracellular NOTCH1. The high prevalence of both mutations indicates the importance of NOTCH1 as a potential therapeutic target for the treatment of T-ALL [8]. Even in the presence of mutations, NOTCH1 activation requires cleavage of the transmembrane protein by the gamma-secretase complex for activation of signaling [9]. Therefore, signaling can be abrogated by inhibition of this catalytic complex with targeted inhibitors [10]. Although gamma-secretase inhibitors effectively inhibit proliferation of T-ALL in vitro and in vivo, clinical development is hampered by dose-limiting on-target induction of severe intestinal goblet cell

hyperplasia as well as by their modest efficacy [11, 12]. The gamma-secretase complex contains either presenilin 1 (PSEN1) or presenilin 2 (PSEN2) as catalytic subunit. In T-ALL, the expression of PSEN2 is suppressed [13], allowing the targeted inhibition of PSEN1-containing complexes, thus avoiding PSEN2-mediated adverse effects [14]. Habets et al. [13] demonstrated that PSEN1-selective targeting of the gamma-secretase complex with MRK-560 is safe and effective for T-ALL. However, an urgent need for drugs that synergistically enhance the antileukemic effects of this class of molecules still remains [15].

The discovery of the BCR-ABL1 fusion kinase in chronic myeloid leukemia prompted the development of the targeted inhibitor imatinib, the first small molecule signal transduction inhibitor approved for clinical use, which greatly improved long-term survival for patients with chronic myeloid leukemia [16]. Similarly, the development of the JAK1/JAK2 kinase inhibitor ruxolitinib was driven by the high prevalence of mutations in JAK2 in myeloproliferative neoplasms. Ruxolitinib could be effective in about 20–30% of T-ALL cases with JAK-STAT pathway activation where JAK1 plays a central signaling role [17]. Similarly, imatinib could be used for rare T-ALL cases with ABL1 fusions, but case reports have shown variable efficacy in this setting [18]. Recently, selective inhibition of nuclear export by the second-generation exportin-1 (XPO1) inhibitor KPT-8602 (eltanexor) was shown to induce apoptosis in various cancer types, including ALL [19, 20], without deleterious effects to normal hematopoiesis [21]. Interestingly, the cancer-specific properties of this small molecule do not require specific mutations and previous studies in ALL have shown a general sensitivity of ALL cells for KPT-8602, independent of any genomic markers [19–21].

Here, we explored synergistic treatment combinations for NOTCH1 or FBXW7 mutated T-ALL in terms of efficacy and tolerance. In a first approach, we added ruxolitinib or imatinib in the presence of JAK3 mutations or the NUP214-ABL1-fusion, respectively. Our second aim was to expand combinatorial targeted therapy to the largest possible number of T-ALL cases by testing the synergy between MRK-560 and KPT-8602, a drug combination that could be effective in all T-ALL cases with activated NOTCH1 signaling. Our results show that the combination of PSEN1-selective gamma-secretase inhibition with a second targeted treatment is highly effective and does not cause additional toxicity.

## Methods

### Cell culture

ALL-SIL, HSB-2, LOUCY, HPB-ALL, DND41, RPMI-8402 and JURKAT cell lines were obtained from DSMZ and cultured in RPMI-1640 medium supplemented with 20% fetal bovine serum (Invitrogen, CA, USA) in 5% carbon dioxide at 37 °C.

**Compounds.** Dimethyl sulfoxide Hybri-Max (D2650), (2-Hydroxypropyl)- $\beta$ -cyclodextrin (H107), Tween-80 (P1754), meglumine (M9179) and methylcellulose (M0262) were purchased from Sigma-Aldrich. MRK-560 was purchased from Tocris Bioscience. KPT-8602 (eltanexor) was bought from Selleckchem. Imatinib mesylate was obtained from AdooQ BioScience (A10468) and ruxolitinib phosphate from MedChem Express (HY-50858).

**Western blotting.** Cell lysates were prepared using 1X Cell Lysis Buffer (Cell Signaling) containing protease inhibitors (cOmplete—EDTA-free, Roche), PhosSTOP (Roche) and 5 mM Na<sub>3</sub>VO<sub>4</sub>. Proteins were separated by SDS-PAGE (NuPAGE NOVEX 4–12% Bis Tris, Invitrogen) and transferred to a nitrocellulose membrane using the Mini Trans-Blot Cell system (Bio-Rad). Labelling was carried out using unlabeled primary antibodies: Cleaved NOTCH1 (#2421, Cell Signaling Technology), PTEN (#9552, Cell Signaling Technology),  $\beta$ -actin (Sigma-Aldrich A1978). Western blot detection was performed with secondary antibodies conjugated with horse-radish peroxidase (GE Healthcare). Images were acquired using a cooled charge-coupled device camera system (ImageQuant LAS-4000, GE Health Care). For cleaved NOTCH1, cells were treated with MRK-560 1  $\mu$ M or PF-03084014 1  $\mu$ M for 24 h prior to lysis.

### Proliferation assays and inhibitor treatment

T-ALL cells were treated with DMSO, single compound or a combination of compounds for up to 14 days. Cells were seeded at a starting concentration of  $3 \times 10^5$  cells per mL and sub-cultured every 2–3 days by centrifugation, resuspension in fresh medium and addition of new compound. Cell concentration and viability were determined by FSC/SSC on a Guava EasyCyte Benchtop Flow cytometer (Merck Millipore). MRK-560 does not cause an immediate effect on cell proliferation and survival, and therefore, pretreatment was used when combined with other drugs in short-term experiments. Seven-day pretreated or untreated cells were seeded in 96-well plates ( $3 \times 10^5$  cells/mL), and compounds (inhibitor or DMSO) were dispersed in a randomized fashion by a D300e digital dispenser (Tecan). Compound concentration was normalized to DMSO. A quantitative evaluation of proliferation was done after 48 h with ATPlite (PerkinElmer)

and measured on the VICTOR X4 Reader (PerkinElmer). Synergy was analyzed using CompuSyn software.

**Apoptosis assay.** Apoptosis was measured after 12 days of treatment with DMSO, single compound or combination with the FITC Annexin V detection kit with PI (Biolegend). Cells were analyzed on a MACSQuant Vyb flow cytometer (Miltenyi Biotec), and data were analyzed using FlowJo Software (Becton, Dickinson and Company).

### Human primary leukemia samples

Primary leukemia samples were obtained at local institutions with informed consent. All experiments were conducted on protocols approved by the ethical committee of the University Hospital Leuven (UZ Leuven).

**Animal studies.** All mouse experiments were approved by the KU Leuven ethical committee and conducted according to EU legislation (Directive 2010/63/EU). NOD.Cg-Prkdc<sup>scid</sup> Il2rg<sup>tm1Wjl</sup>/Sz (NSG) mice used for patient-derived xenograft experiments were bred in-house or purchased from Charles River Laboratories. During experiments, mice were housed in individually ventilated cages enriched with wood wool and shavings as bedding, with access to water and food *ad libitum* and monitored daily. Disease progression was monitored by weekly facial vein blood sampling followed by red blood cell lysis and staining with anti-hCD45-APC (#368512, BioLegend) for flow cytometry analysis (MACS Quant VYB, Miltenyi). After confirmation of engraftment, mice were randomized into treatment arms and treated according to protocol. For survival experiments, the presence of > 50% human CD45+ cells in the peripheral blood was used as surrogate end-point for leukemia-related death, and animals were subsequently euthanized (based on ethical guidelines). MRK-560 (30  $\mu$ mol/kg) was dissolved in 20% hydroxypropyl- $\beta$ -cyclodextrin (HP- $\beta$ -CD) in 0.1 M meglumine for administration by intraperitoneal injection or 40% HP- $\beta$ -CD in 0.3 M meglumine for oral gavage. KPT-8602 (5 mg/kg) was dissolved in 0.5% methylcellulose with 1% Tween-80 for oral gavage. Ruxolitinib (90 mg/kg) and imatinib (100 mg/kg) were dissolved in 0.5% methylcellulose and administered via oral gavage. In vivo treatment period was set at 2 weeks initially and extended to 3 weeks for later experiments to achieve a stronger response.

### Patient-derived xenografts

Primary cells were injected into the tail vein of 6- to 8-week-old female NSG mice. After successful engraftment, splenocytes were harvested and  $1 \times 10^6$  cells were injected into secondary recipient mice for treatment. Selected samples were transduced with the lentiviral pCH-SFFV-eGFP-T2A-fLuc vector and sorted for

GFP-positivity using an S3e Cell Sorter (Bio-Rad) prior to reinjection into NSG mice.

#### **In vivo bioluminescence imaging**

Mice were anesthetized with 2% isoflurane in 100% oxygen, injected subcutaneously with D-luciferin (126 mg/kg, Promega) dissolved in PBS (15 mg/mL) and placed in an IVIS Spectrum (Caliper Life Sciences) while maintaining anesthesia. Consecutive 2-min frames were acquired. Results are reported as maximum total flux per second for each whole mouse.

#### **Immunohistochemistry**

After collection, tissues were fixed in 10% neutral buffered formalin (Sigma) for 48 h followed by processing for paraffin embedding (HistoStar Embedding Workstation). Sections of 7  $\mu$ m thickness from the paraffin-embedded tissues (Thermo Scientific Microm HM355S microtome) were mounted on Superfrost Ultra Plus Adhesion slides (Thermo Scientific) and routinely stained with hematoxylin and eosin (Mayers Haematoxylin 1 l, 3801582E, Leica; Eosin Y solution, aqueous (1 L), HT110232-1L, Sigma-Aldrich) for histopathological examination. Then, sections were stained with periodic acid–Schiff (PAS). Slides were incubated in freshly prepared periodic acid (0.5%) for 15 min, rinsed, and incubated for 5 min in distilled water. The Schiff reagent (3952016-500ML, Sigma-Aldrich) was added onto the slides and kept for 15 min at room temperature in dark. The sections were then washed in slightly lukewarm running tap water for 5 min, rinsed and incubated in distilled water for 2 min, and counterstained in Mayer's hematoxylin for 1 min. After washing in running tap water for 5 min, sections were dehydrated (95% EtOH, 100% EtOH, 100% EtOH, 3 min each, followed by two times xylene for 5 min) and mounted in DPX mounting medium (06,522, Sigma).

#### **Microscope image acquisition and image processing**

Images were acquired on the Zeiss Axio Scan.Z1 using an  $\times 20$  objective and ZEN 2 software. For exporting images, the ZEN 2 software (Zeiss) was used. Analysis was performed with QuPath software.

#### **Statistical analyses**

For analysis of synergy, the Chou-Talalay method was used, using CompuSyn software (ComboSyn, Inc). Graphs are presented as mean  $\pm$  standard deviation unless stated otherwise, and all analyses were performed using GraphPad Prism. Comparison between two groups was made by the Student's unpaired two-tailed *t*-test. One-way ANOVA with Bonferroni correction for multiple comparisons was used to examine differences when comparing effects in three or more groups. Survival in

mouse experiments was represented with Kaplan–Meier survival curves, and statistical significance was calculated using the log-rank (Mantel Cox) test.

## **Results**

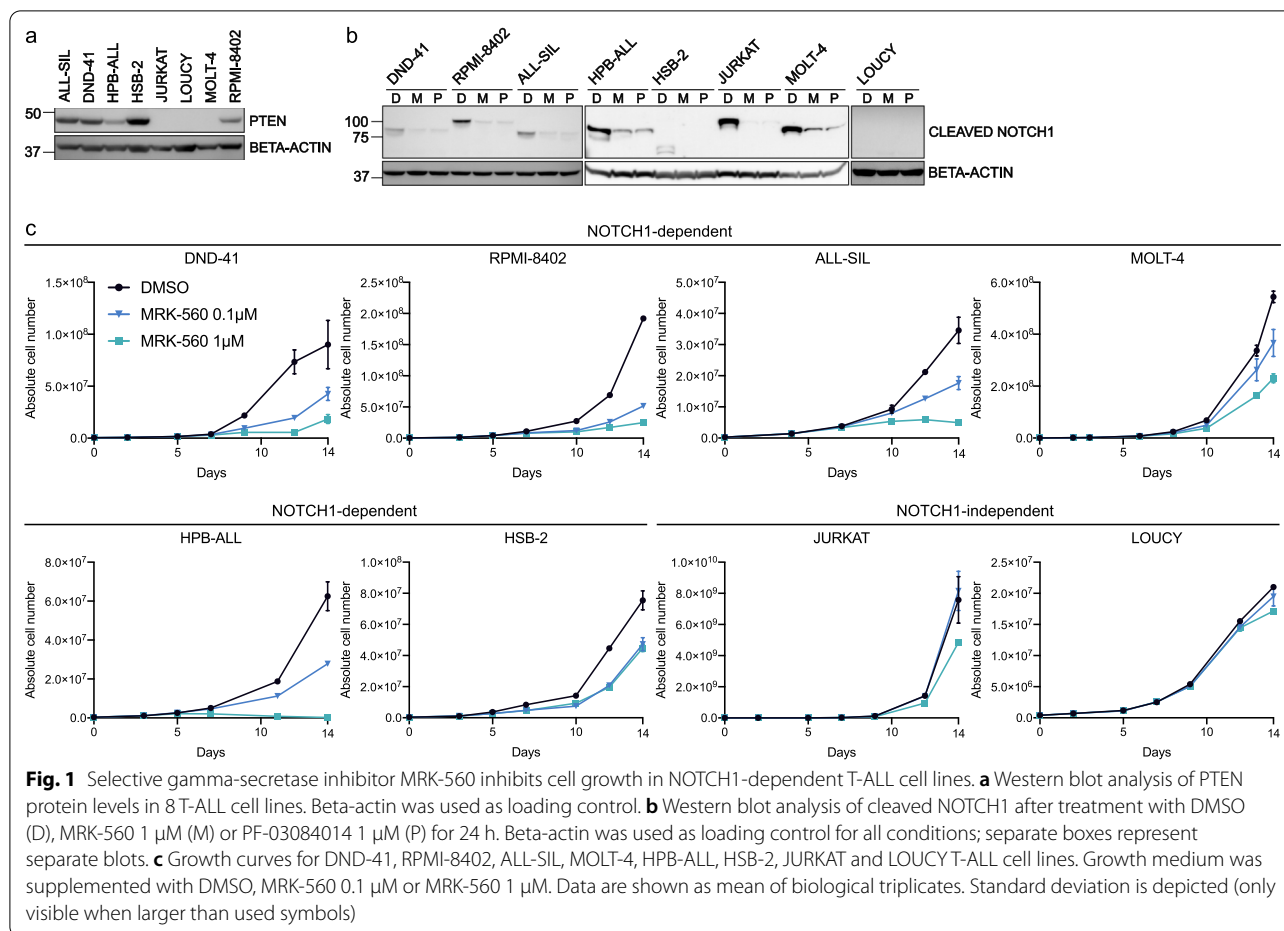
### **Selective gamma-secretase inhibitor MRK-560 impairs cell growth in NOTCH1-dependent cells**

We tested the sensitivity to PSEN1-selective gamma-secretase inhibitor MRK-560 [22] in 6 NOTCH1-dependent and 2 NOTCH1-independent cell lines (JURKAT cells have a NOTCH1 mutation but are independent of NOTCH1 signaling due to AKT pathway activation and LOUCY has no NOTCH1 pathway mutations). Mutations in NOTCH1 and FBXW7 were confirmed using Sanger sequencing (Additional file 1: Table S1), and the presence of cleaved NOTCH1 and the PTEN protein was verified by Western blot analysis (Fig. 1a, b). In these cell lines, MRK-560 inhibited the formation of cleaved NOTCH1 to the same extent as the non-selective gamma-secretase inhibitor PF-03084014 [11, 23] (Fig. 1b). MRK-560 treatment caused a dose-dependent inhibition of proliferation/survival in cell lines that depend on NOTCH1 signaling (Fig. 1c). Together, these data indicate that MRK-560 is a potent inhibitor of NOTCH1 signaling with comparable activity as broad gamma-secretase inhibitors.

It has previously been suggested that FBXW7 mutations or PTEN loss can confer resistance to gamma-secretase inhibitors [24, 25]. However, treatment with MRK-560 strongly impaired cell growth of HPB-ALL and RPMI-8402 cells, which carry mutations in both NOTCH1 and FBXW7. Similar effects were observed for HSB-2 cells, a FBXW7 mutated and NOTCH1 wild-type cell line. Moreover, of the three cell lines that lack the PTEN protein, MOLT-4 was still sensitive to MRK-560. This supports previous observations that aberrations in FBXW7 or PTEN do not imperatively relieve T-ALL of its NOTCH1 addiction [26].

### **Combining MRK-560 with tyrosine kinase inhibitors synergistically inhibits proliferation**

To test whether we could achieve synergistic activity when combining MRK-560 with other inhibitors, we focused on the genetic background of T-ALL. NOTCH1 and FBXW7 mutations are distributed evenly throughout the different genetic subgroups of T-ALL and, therefore, often co-occur with other targetable aberrations. Interleukin-7 (IL7) signaling activating mutations affect about one-third of T-ALL patients [8, 27] and occur in every component of the signaling pathway: the receptor  $\alpha$ -chain IL7R, kinases JAK1 and JAK3 or the transcription factor STAT5 and the subsequent pathway activation can be inhibited by JAK-inhibitors [28, 29]. T-ALL cell



line DND-41 depends on IL7 signaling due to a mutation in the IL7R gene, which is reflected in its sensitivity to the JAK kinase inhibitor ruxolitinib (Fig. 2a).

To examine the combined effect of MRK-560 and ruxolitinib, we cultured the cells for 14 days in medium supplemented with either MRK-560 (100 nM) or ruxolitinib (1  $\mu$ M) alone or together. The drug combination induced a greater reduction in proliferation than single-drug treatment for DND-41, but not in the control cell lines RPMI-8402 and LOUCY, supporting the on-target effects of ruxolitinib and MRK-560 (Fig. 2b). Additionally, 7-day pretreatment with MRK-560 enhanced the efficacy of JAK kinase inhibition, yielding a significantly lower cell viability than with single-drug treatment (Fig. 2c) and increased apoptosis (Fig. 2d). Pretreatment with MRK-560 was used as this drug does not induce immediate effects on proliferation or survival. Calculation of combination indices (CI) revealed that the combination of both inhibitors was synergistic and affected a large fraction of the treated cells (Fig. 2e).

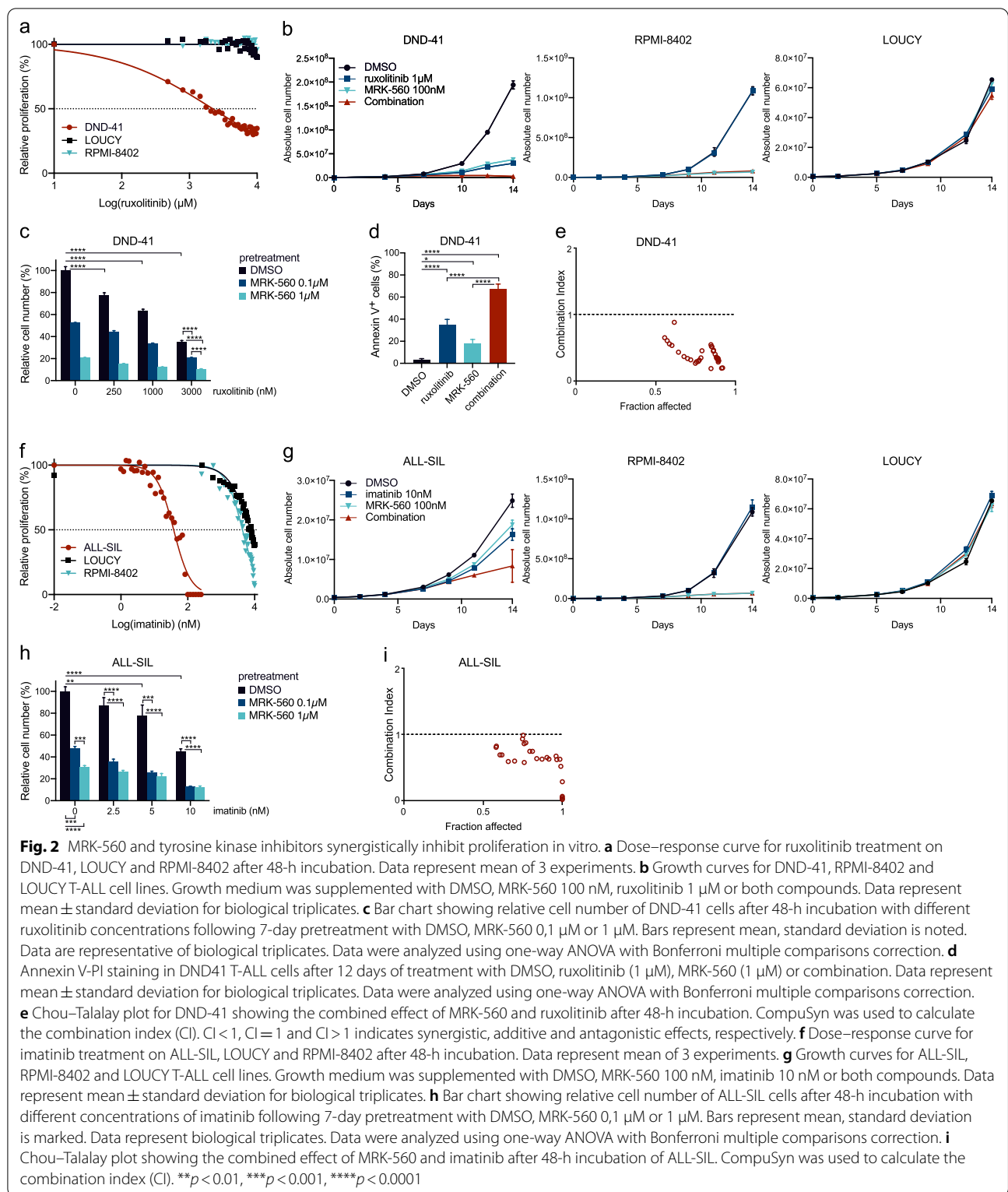
We applied a similar approach for fusions containing the ABL1 tyrosine kinase. NUP214-ABL1 is the most

frequent ABL1 fusion gene in T-ALL (6% of T-ALL cases) [30] and other (rare) fusions are ETV6-ABL1, BCR-ABL1, ZBTB16-ABL1 and EML1-ABL1 [6, 31]. ALL-SIL carries the NUP214-ABL1 fusion, which makes it sensitive to ABL1-kinase inhibitor imatinib [5] (Fig. 2f). When cultured in the presence of MRK-560 (100 nM) and imatinib (10 nM), ALL-SIL showed a much greater proliferation deficit when both inhibitors were combined (Fig. 2g). Pretreatment of ALL-SIL with MRK-560 for 7 days strongly increased the effect of imatinib (Fig. 2h), even at low concentrations, and the nature of this drug cooperation was clearly synergistic (Fig. 2i).

#### **In vivo combination of MRK-560 with tyrosine kinase inhibition reduces leukemic bone marrow infiltration**

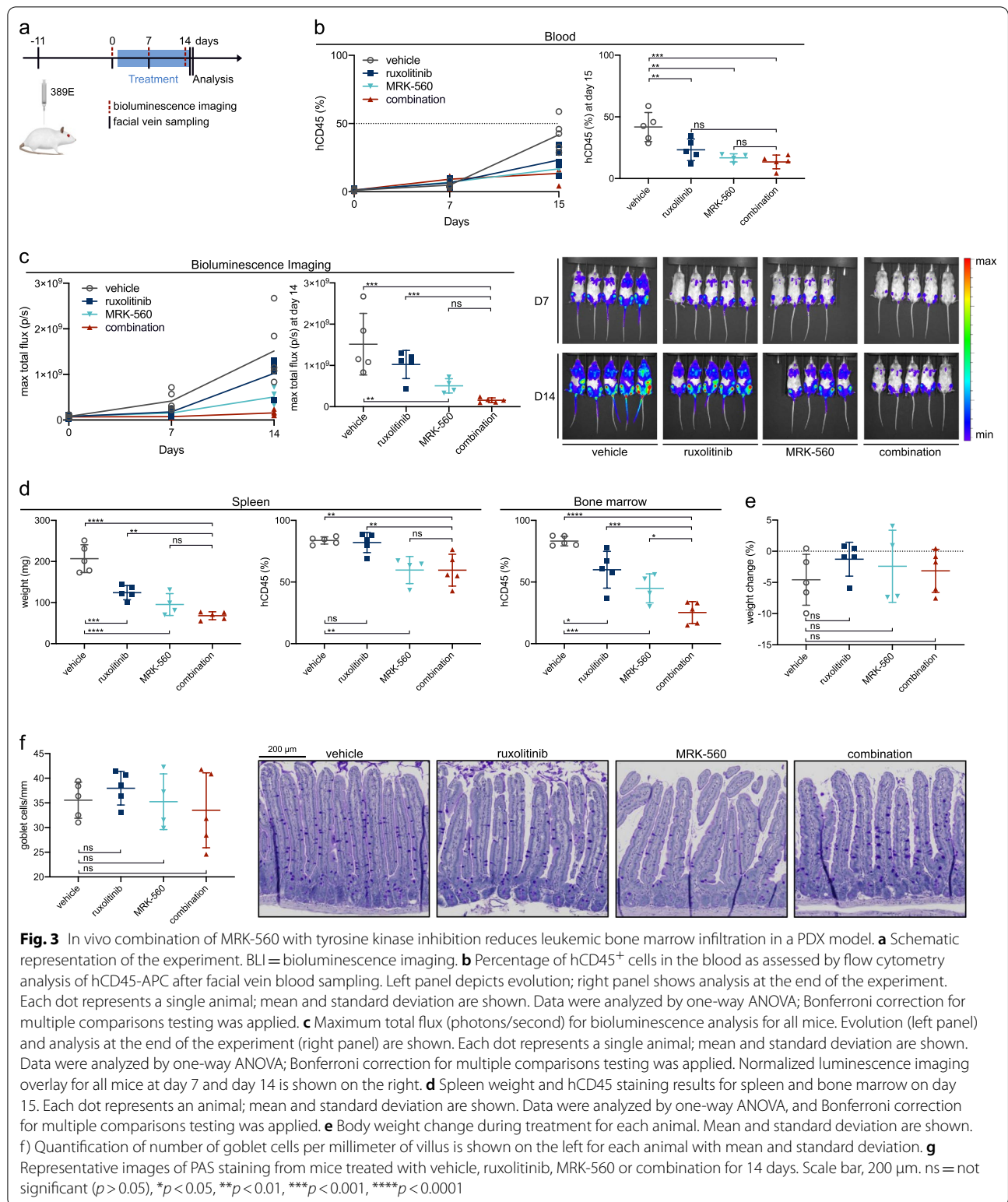
To verify and extend the preclinical value of our in vitro data, we set up in vivo validation experiments in a patient-derived xenograft (PDX) model. Patient sample 389E was derived from a T-ALL patient with mutations in NOTCH1 and JAK3 (Additional file 2: Table S2). The sample was injected into 20 NOD.Cg-Prkdc<sup>scid</sup> Il2rg<sup>tm1Wj</sup>/SzJ (NSG) immunodeficient mice via tail vein





injection. After engraftment, mice were randomized to vehicle, MRK-560 [30  $\mu$ mol/kg, intraperitoneal injection (IP)], ruxolitinib [90 mg/kg, oral gavage (PO)] or

combination treatment and were treated for 14 days (Fig. 3a). Although leukemia progression was effectively reduced in all treatment conditions when assessed by



blood count of human CD45<sup>+</sup> (hCD45<sup>+</sup>) cells, the combination arm did not have significantly less leukemic cells in the blood after 14 days of treatment (Fig. 3b). However, when global disease burden was measured using in vivo

bioluminescence imaging (BLI), the combination outperformed ruxolitinib-only treatment (Fig. 3c). Analysis of the mice after the 2-week treatment period revealed a significantly smaller spleen size, associated with reduced

leukemic infiltration (Fig. 3d), for all treatment groups when compared to vehicle-treated mice. Adding MRK-560 to ruxolitinib clearly increased the efficacy of JAK-inhibition, but results were not better than MRK-560 alone. In contrast, the bone marrow was significantly less infiltrated by leukemic cells in the combination treatment. Importantly, no signs of increased gastrointestinal toxicity were noted in the mice. We did not observe pathological changes in the gut architecture. The abundance of goblet cells was assessed by periodic acid-Schiff (PAS) staining and was unaltered by the treatment, resulting in similar weight changes for all treatment groups (Fig. 3e, f).

**In vivo sensitivity to PSEN1-selective gamma-secretase inhibition of an FBXW7 mutated PDX is enhanced by addition of imatinib**

We showed that, in vitro, FBXW7-mutated T-ALL can be sensitive to gamma-secretase inhibition (Fig. 1c). To test this in vivo, we used PDX sample X12, which contains an inactivating mutation in FBXW7 and a

NUP214-ABL1 fusion gene. After engraftment into NSG mice, animals were randomized and treated with MRK-560 (30 µg/kg, PO) and/or imatinib (100 mg/kg, PO) or vehicle (Fig. 4a). Due to the aggressive nature of this sample, mice could only be treated for 12 days after confirmed engraftment before vehicle-treated animals needed to be euthanized. After 7 days of treatment, disease progression was slowed down in treatment groups receiving MRK-560, which supports in vivo sensitivity of FBXW7-mutated T-ALL to NOTCH1 inhibition. Despite the short treatment duration, hCD45<sup>+</sup> blood counts were significantly reduced in the mice that received the combination treatment (Fig. 4b). Treatment with MRK-560 reduced spleen size, and the addition of imatinib significantly enhanced the reduction in spleen infiltration compared to MRK-560 alone (Fig. 4c). This superior effect on tissue infiltration was reflected in the bone marrow, where only the combination of MRK-560 and imatinib effectively reduced the leukemia burden.

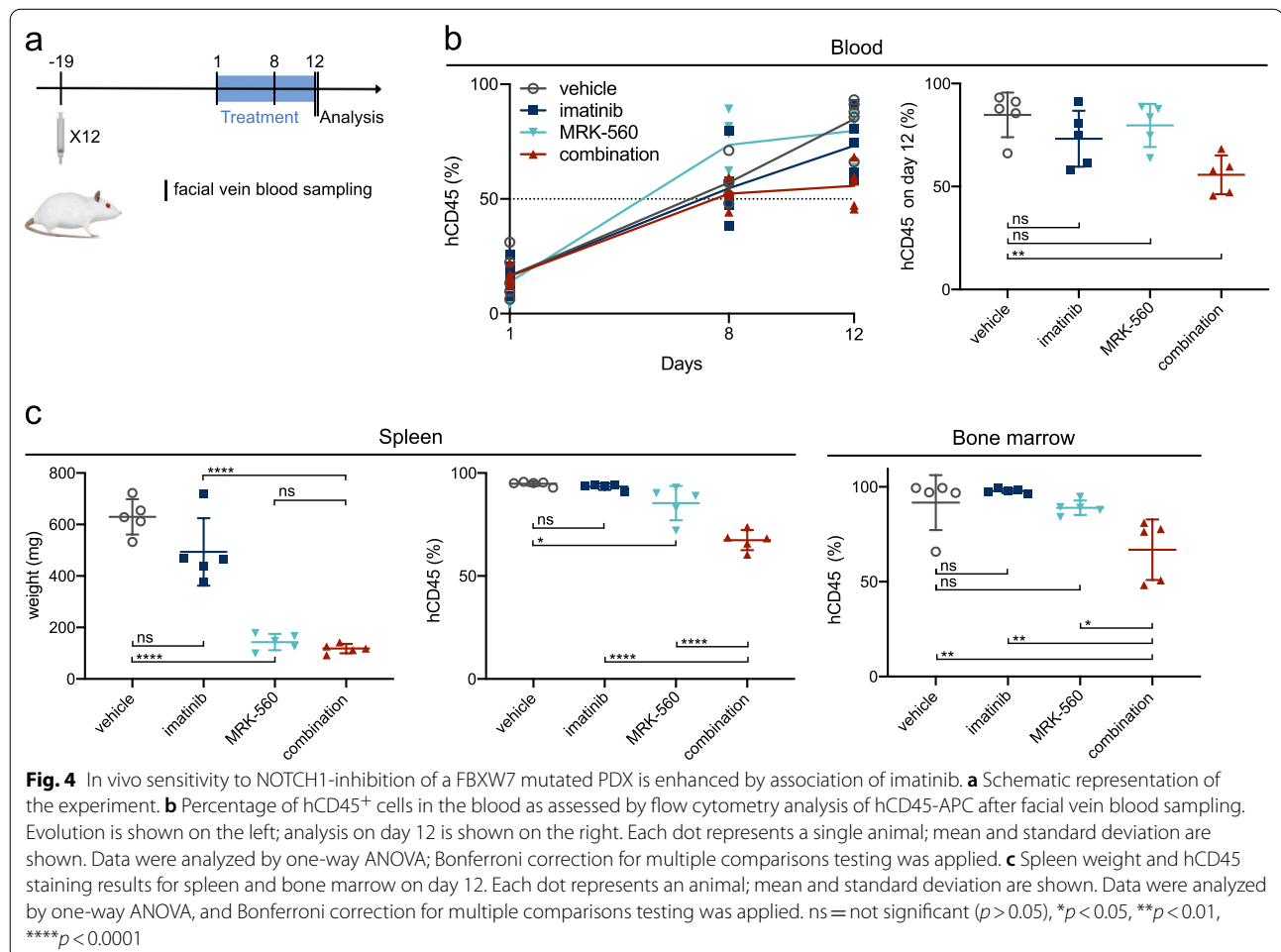


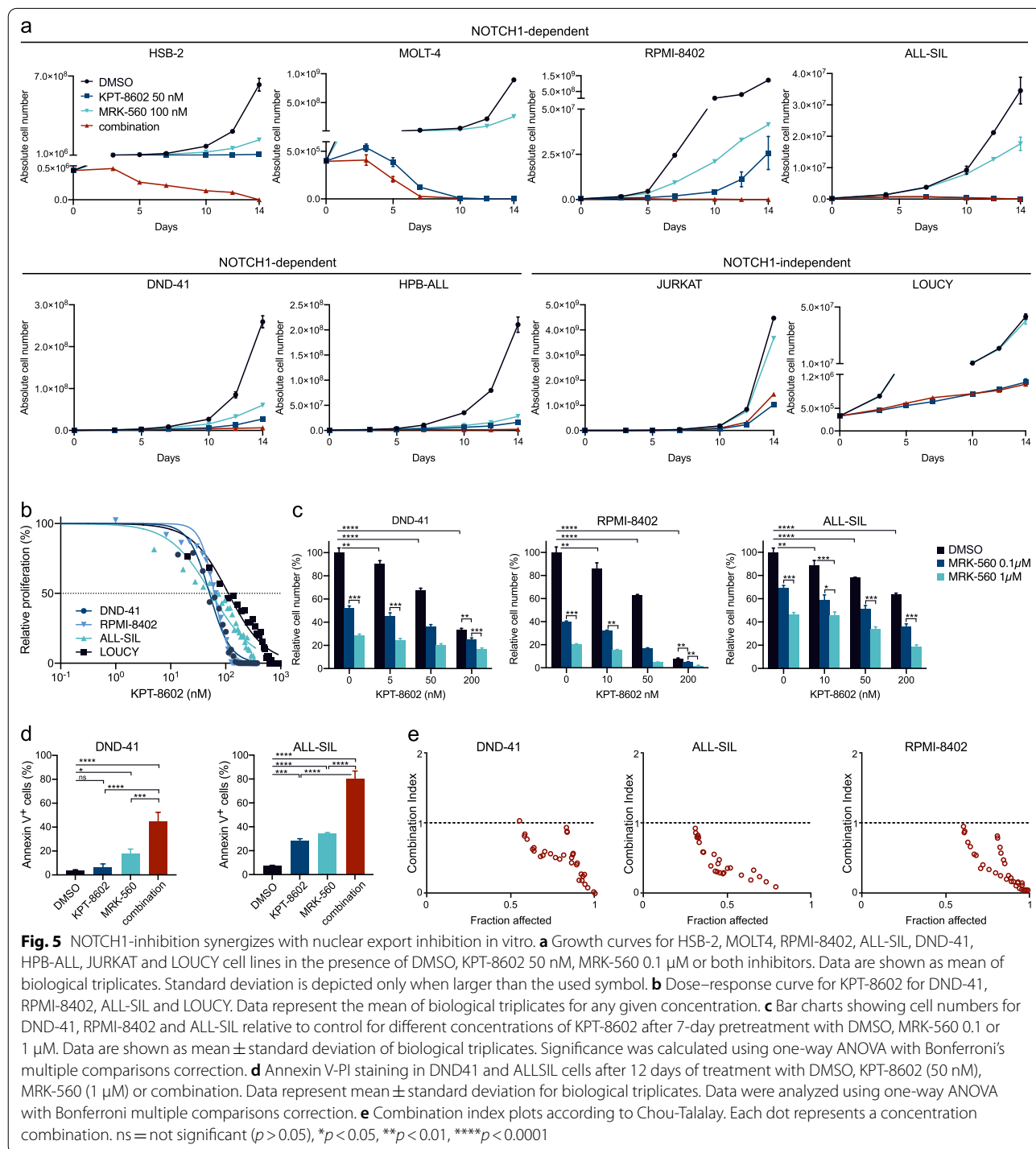
**Fig. 4** In vivo sensitivity to NOTCH1-inhibition of a FBXW7 mutated PDX is enhanced by association of imatinib. **a** Schematic representation of the experiment. **b** Percentage of hCD45<sup>+</sup> cells in the blood as assessed by flow cytometry analysis of hCD45-APC after facial vein blood sampling. Evolution is shown on the left; analysis on day 12 is shown on the right. Each dot represents a single animal; mean and standard deviation are shown. Data were analyzed by one-way ANOVA; Bonferroni correction for multiple comparisons testing was applied. **c** Spleen weight and hCD45 staining results for spleen and bone marrow on day 12. Each dot represents an animal; mean and standard deviation are shown. Data were analyzed by one-way ANOVA, and Bonferroni correction for multiple comparisons testing was applied. ns = not significant ( $p > 0.05$ ), \* $p < 0.05$ , \*\* $p < 0.01$ , \*\*\*\* $p < 0.0001$



**PSEN1-selective gamma-secretase inhibition synergizes with nuclear export inhibition in vitro**

Because selective inhibitors of nuclear export do not require a mutated target and were shown to inhibit the growth of all subtypes of ALL, combination of KPT-8602 and MRK-560 could potentially benefit all T-ALL

patients with activated NOTCH1 signaling. To test whether MRK-560 and KPT-8602 act synergistically, we cultured T-ALL cell lines for 14 days in the presence of DMSO, MRK-560 (100 nM), KPT-8602 (50 nM) or both inhibitors (Fig. 5a). All cell lines were sensitive to KPT-8602, independent of NOTCH1 or FBXW7 status. For



(See figure on next page.)

**Fig. 6** Combination of MRK-560 and KPT-8602 reduces leukemia burden in vivo. **a** Schematic representation of the experiment. **b** Percentage of hCD45<sup>+</sup> cells in the blood as assessed by flow cytometry analysis of hCD45-APC after facial vein blood collection over time (left) and at day 15 (right). Each dot represents a single animal; mean and standard deviation are shown at day 15. Data were analyzed by one-way ANOVA; Bonferroni correction for multiple comparisons testing was applied. **c** Bioluminescence imaging results for all mice, measured as maximum total flux (photons/second). Evolution over time (top) and analysis at day 14 (bottom, left) of the experiment are shown. Each dot represents a single animal; bars represent mean and standard deviation. Fold change in maximum total flux between end and start of treatment was calculated for each mouse (bottom, middle). Data were analyzed by one-way ANOVA; Bonferroni correction for multiple comparisons testing was applied. Normalized luminescence imaging overlay for all mice at days 0, 7, and day 14 is shown on the right panel. **d** Spleen weight and hCD45 staining results for spleen and bone marrow on day 15. Each dot represents an animal; mean and standard deviation are shown. Data were analyzed by one-way ANOVA, and Bonferroni correction for multiple comparisons testing was applied. **e** Kaplan–Meier plot showing survival for the remaining 5 mice in every treatment group. Gray area indicates treatment period. **f** Body weight change during treatment for each animal (top) and quantification of number of goblet cells per millimeter of villus (bottom) ( $n=3$ ). Mean and standard deviation are shown. **g** Representative images of PAS staining from mice treated with vehicle, KPT-8602, MRK-560 or combination for 14 days. Scale bar, 200  $\mu\text{m}$ . ns = not significant ( $p > 0.05$ ), \* $p < 0.05$ , \*\* $p < 0.01$ , \*\*\* $p < 0.001$ , \*\*\*\* $p < 0.0001$

NOTCH1-dependent cells, the combination of both inhibitors was highly effective, strongly inhibiting leukemia proliferation and/or inducing cell death. This could not be achieved with single-drug treatment, except in MOLT-4 where the combination accelerated the effect of KPT-8602. We selected 3 cell lines with similar sensitivity to KPT-8602 (Fig. 5b), to study the cooperation between these compounds. Seven days of pretreatment with MRK-560 increased sensitivity to KPT-8602, resulting in significantly lower proliferation/viability (Fig. 5c) and increased apoptosis (Fig. 5d). For the majority of the tested concentrations, the combination of MRK-560 with KPT-8602 was synergistic ( $CI < 1$ ) (Fig. 5e).

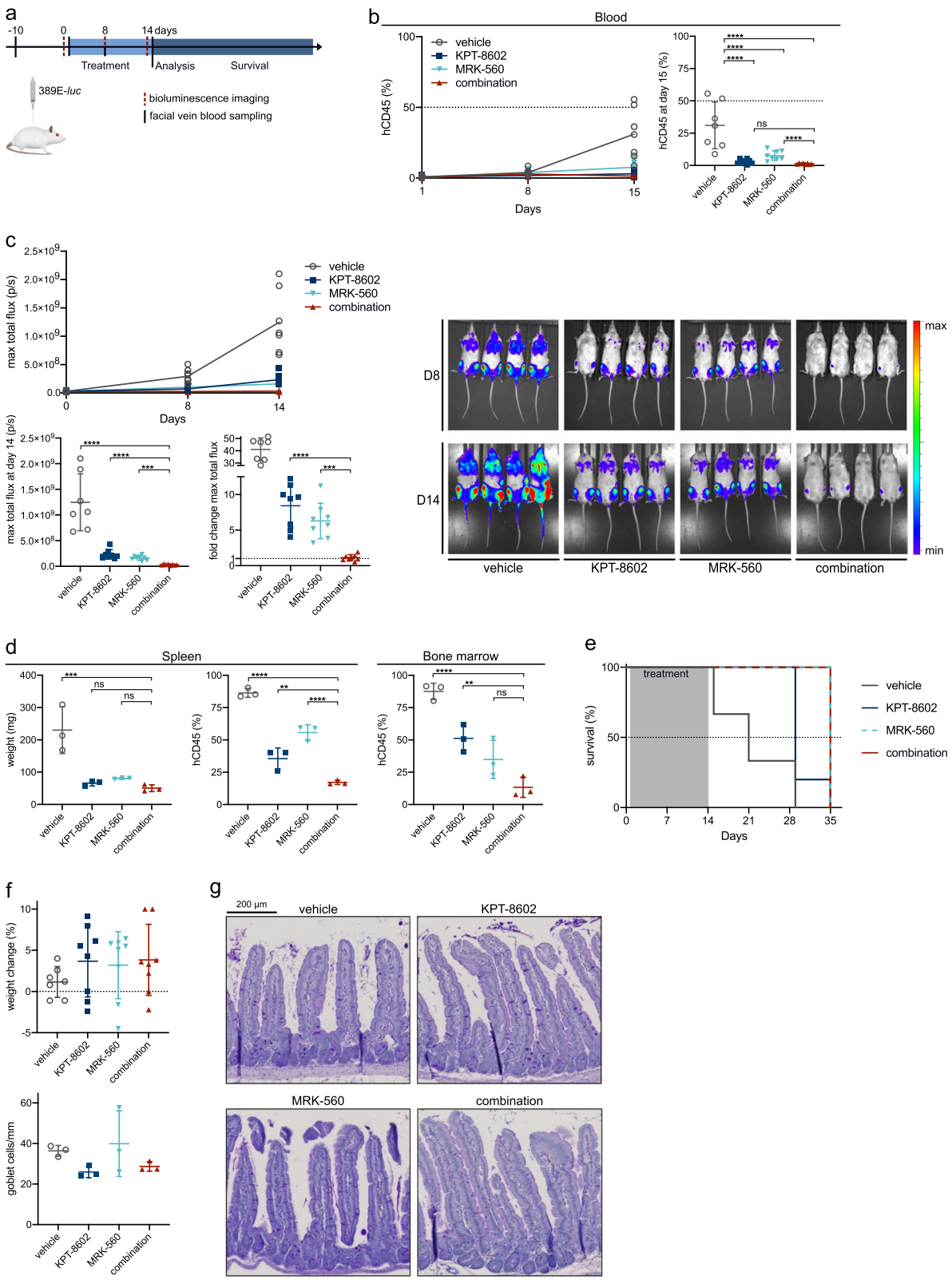
#### **Leukemia burden is reduced in vivo when MRK-560 and KPT-8602 are combined**

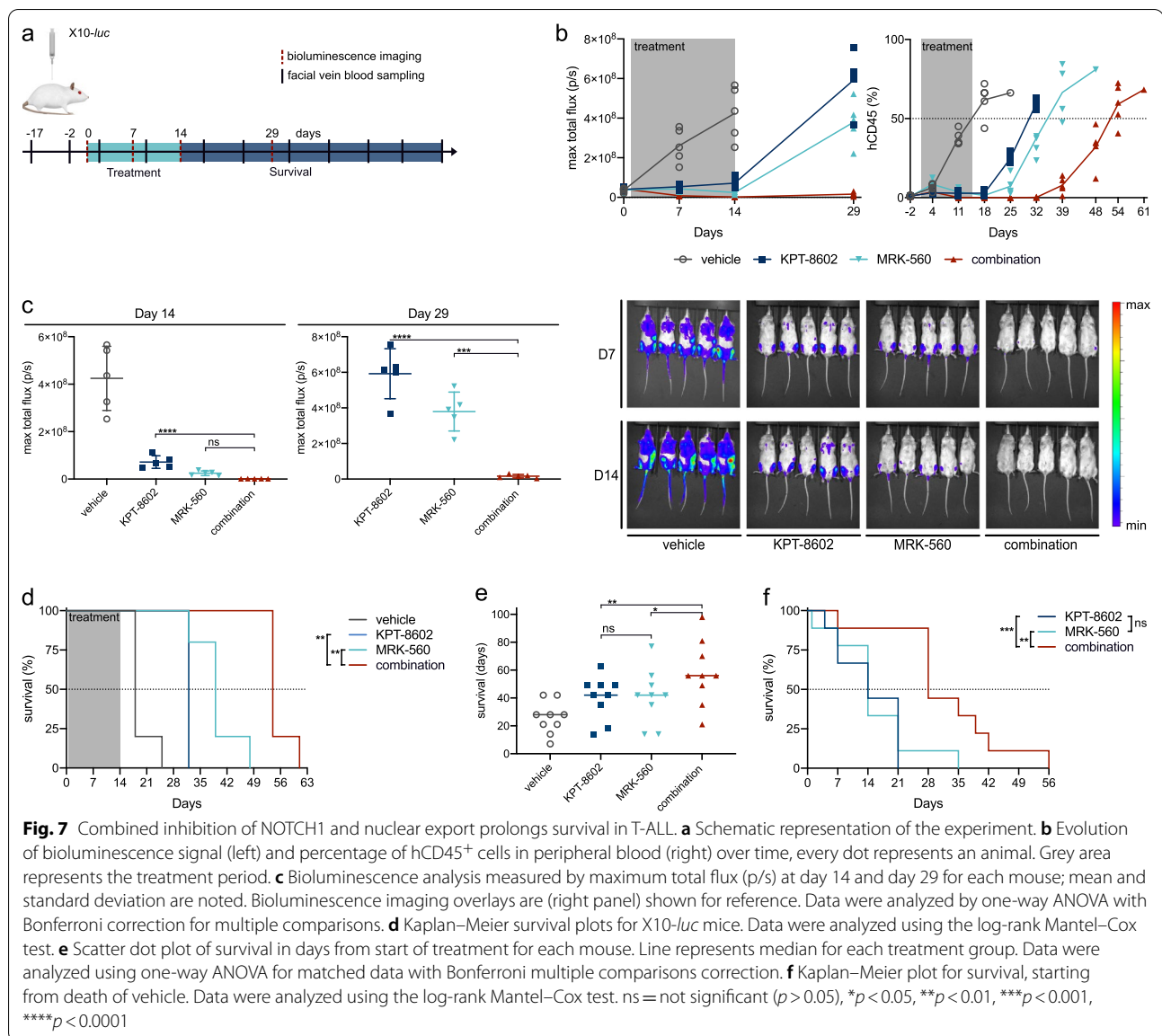
For in vivo validation, we injected 32 NSG mice with NOTCH1- and JAK3-mutated PDX sample 389E. After engraftment and randomization, mice were treated for 14 days with vehicle, KPT-8602 (5 mg/kg, PO), MRK-560 (30  $\mu\text{g}/\text{kg}$ , IP) or both compounds (Fig. 6a). hCD45<sup>+</sup> lymphoblasts in the blood were effectively reduced in both single-drug treatment arms and nearly eradicated in the animals treated with the combination (Fig. 6b). The difference between KPT-8602-only treatment and combination did not reach significance in the blood. However, systemic evaluation of leukemia burden by bioluminescence imaging clearly showed superiority of combination treatment (Fig. 6c). Single-drug treatment significantly slowed down leukemia development, but to a lesser extent than combination treatment. After 14 days of treatment, 50% of the mice in the combination condition had maximum total flux values below their starting value, as represented by the fold change  $< 1$  (range 0.52–1.93). Subsequently, 3 mice were randomly selected from every group and were euthanized for tissue analysis. None of the treated mice developed splenomegaly, but

the mice from the combination arm showed significantly less leukemic infiltration in the spleen, when compared to single-treatment arms (Fig. 6d). Bone marrow disease was reduced, but the difference in bone marrow infiltration was not significant. As a consequence, combination treatment did not yield a survival benefit (Fig. 6e). None of the mice developed goblet cell hyperplasia or significant weight loss (Fig. 6f, g).

#### **Combined inhibition of PSEN1-gamma-secretase and nuclear export prolongs survival in T-ALL**

To study whether the observed reduction in measurable leukemic disease could improve survival nonetheless, we set up a survival experiment with patient sample X10-luc. Twenty NSG mice were randomized and treated for 14 days with the same regimen as described for 389E (Fig. 7a). Disease progression and efficacy of treatment were followed by BLI and measurement of hCD45 in peripheral blood (Fig. 7b, c). The presence of  $> 50\%$  hCD45<sup>+</sup> cells in the blood was considered as surrogate endpoint for death due to leukemia. At the end of the 14-day treatment period, global disease burden as measured by bioluminescence was strongly reduced in all treated mice, without a significant benefit of combination treatment over MRK-560 monotherapy (Fig. 7c). Nevertheless, when treatment was stopped, we noted an early flare-up of the disease in the animals from the single-drug treatment arms, and by days 29 and 32, respectively, the bioluminescence and hCD45<sup>+</sup> levels had risen to those of untreated mice. In contrast, in the mice receiving the combination treatment, the disease remained suppressed, and at day 29 (BLI) or day 32 (blood analysis) disease levels were still lower than at the start of the treatment (Fig. 7b, c). This prolonged suppression of T-ALL resulted in a significantly longer survival for the animals in the combination group when compared to





MRK-560 (1.4-fold,  $p = 0.002$ ) and KPT-8602 (1.69-fold,  $p = 0.0027$ ) (Fig. 7d).

To evaluate whether these results could be confirmed in a broader cohort of NOTCH1- or FBXW7-mutated T-ALL patients, we set up a drug treatment trial with nine different PDX samples. Two samples (XD83 and XD83q) were a matched diagnosis–relapse pair derived from the same patient. Each sample was injected into four NSG mice, and mice were randomized so that every treatment group contained 1 mouse for every PDX sample. Mutations for all PDXs were verified by Sanger sequencing and are listed in Additional file 2: Table S2. This approach allowed us to run a small-scale clinical trial-like experiment to validate the predicted

survival benefit in a cohort of PDX samples, each with its own mutational background and proliferation rate.

Because of the delayed effect of MRK-560 (Fig. 4b, 7b) on hCD45<sup>+</sup> blood levels in some of the treated mice in earlier experiments, we used here a treatment period of 3 weeks (5 days on, 2 days off treatment). Blood was sampled every week, and the presence of more than 50% hCD45<sup>+</sup> cells was considered as surrogate endpoint for survival. Median survival was 28 days for vehicle treated mice, 42 days for mice that received single-drug treatment and 56 days for the mice in the combination treatment arm. Mice in all treatment arms lived longer than vehicle-treated mice. Four out of 9 vehicle-treated mice succumbed during the treatment,

as compared to 2 mice for single-drug treatment and 1 for the combination group, reflecting the aggressiveness of the selected PDX samples and supporting both the efficacy and tolerability of the treatment regimen.

We observed no difference in survival between the two single-drug groups ( $p > 0.9999$ ). However, the mice that were treated with both compounds together lived significantly longer than those treated with MRK-560 only ( $p = 0.0142$ ) or KPT-8602-only ( $p = 0.0058$ ) (Fig. 7e). As expected, a large variability in the rate of disease progression was observed between the different PDX samples with survival ranging from 7 to 42 days from the start of treatment for the vehicle-treated mice. Therefore, we plotted survival as the number of days that mice in the treatment groups outlived their vehicle-treated counterpart (Fig. 7f). Survival curves for KPT-8602 and MRK-560 treated mice were similar ( $p = 0.856$ ), and both treatment groups outlived their vehicle-treated littermate with a median of 14 days. This survival benefit was twice as long in the combination group, resulting in a clear separation between survival curves ( $p = 0.0005$  vs KPT-8602;  $p = 0.0049$  vs MRK-560), supporting the added benefit of combining nuclear export inhibition with gamma-secretase inhibition in T-ALL.

## Discussion

It is unlikely that a single molecule will be able to cure T-ALL. Combining inhibitors could improve efficacy, if done in a rational manner. Targeting NOTCH1 signaling offers the opportunity to target about 70% of T-ALL patients, without subtype restriction [8]. Different approaches for successful NOTCH1 inhibition are under evaluation: interference with NOTCH1 maturation by SERCA-inhibition, NOTCH-targeting inhibitory antibodies and more conventional targeted inhibitors. For the latter, very few gamma-secretase inhibitors have progressed past early-phase clinical studies [11, 12, 32], and none have made it to clinical practice because of dose-limiting toxicity or lack of clinical benefit. As a consequence, there are currently no clinical trials with a gamma-secretase inhibitor ongoing for T-ALL.

Here, we present an extensive preclinical characterization of the PSEN1-selective gamma-secretase inhibitor MRK-560. MRK-560 potently inhibits the proliferation of lymphoblasts both in vitro and in vivo in PDX models. Moreover, we show that MRK-560 reduces leukemic tissue infiltration and prolongs survival without the characteristic gastrointestinal toxicity of non-selective gamma-secretase inhibitors. We also show that sensitivity to MRK-560 is not limited to NOTCH1 mutated cases but can extend to patients carrying mutations in FBXW7.

To increase efficacy, we combined MRK-560 with imatinib or ruxolitinib, inhibitors with a long-standing

experience in clinical practice. We show that the combination of MRK-560 with these inhibitors is synergistic and effectively counters leukemia progression and reduces tissue infiltration in vivo. Importantly, even in short-term experiments, combination treatment provided a clear benefit in the bone marrow niche, suggesting a protective effect against relapse. Finally, the strongest effect was noted in the combination of MRK-560 with nuclear export inhibitor KPT-8602, which makes it possible to obtain the maximum treatment effect in the largest possible cohort, since the majority of T-ALL cases harbor NOTCH1 pathway mutations and no specific mutations are required for sensitivity toward KPT-8602. The association of these two compounds provided a survival benefit across different genetic backgrounds in our PDX models. Although our treatment experiments are limited in terms of animal numbers, the results are consistent over the different genetic backgrounds of the PDX samples. We provide substantial preclinical data to support the development and validation of PSEN1-selective gamma-secretase inhibitors for the treatment of a wide range of T-ALL patients. To conclude, we show that the antileukemic effect of gamma-secretase inhibition can be safely maximized by well-orchestrated combination of small molecule inhibitors providing the rationale for further investigation of PSEN1-selective gamma-secretase inhibitor-based treatment regimens.

## Abbreviations

BLI: Bioluminescence imaging; PAS: Periodic acid–Schiff; PDX: Patient-derived xenograft; T-ALL: T cell acute lymphoblastic leukemia.

## Supplementary Information

The online version contains supplementary material available at <https://doi.org/10.1186/s13045-021-01114-1>.

**Additional file 1.** Supplemental Table 1 describing the cell lines used.

**Additional file 2.** Supplemental Table 2 describing the PDX models used.

## Acknowledgements

We thank Prof. Christine Harrison and the UK Biobank for providing a few of the ALL samples that were used as PDX in this project.

## Authors' contributions

JC and IG designed the study. IG, CP, OG, KJ, SP, DN, CV performed experiments and analyzed data. HS, JM, NB collected ALL samples and analyzed and interpreted patient data. IG and JC wrote the manuscript and CP, CV, JM, KDK provided additional input for the manuscript. All authors read and approved the manuscript.

## Funding

This study was funded by Kom op tegen Kanker (Stand up to Cancer), the Flemish cancer society (to JC); by KU Leuven grant C14/18/104 (to KDK, JC, HS, JM, NB); by fellowships from the FWO to IG and CP. The funders did not have any role in the design of the study, the collection, analysis, and interpretation of data and in writing of the manuscript.



**Availability of data and materials**

Cell lines used in this study are commercially available from [www.dsmz.de](http://www.dsmz.de). PDX samples used in this study can be obtained upon request. No datasets were generated in this study.

**Declarations****Ethics approval and consent to participate**

The collection and use of human ALL samples was approved by the ethical committee from UZ Leuven. The use of immune deficient mice was approved by the ethical committee on animal experiments from KU Leuven.

**Consent for publication**

Not applicable.

**Competing interests**

The authors declare that they have no competing interests.

**Author details**

<sup>1</sup>Center for Human Genetics, KU Leuven, Leuven, Belgium. <sup>2</sup>Center for Cancer Biology, VIB, Leuven, Belgium. <sup>3</sup>Leuvens Kanker Instituut (LKI), KU Leuven – UZ Leuven, Leuven, Belgium. <sup>4</sup>Department of Hematology, UZ Leuven, Leuven, Belgium. <sup>5</sup>Department of Microbiology, Immunology and Transplantation, KU Leuven, Leuven, Belgium. <sup>6</sup>Department of Laboratory Medicine, UZ Leuven, Leuven, Belgium. <sup>7</sup>Department of Oncology, KU Leuven, Leuven, Belgium. <sup>8</sup>Department of Pediatric Oncology, UZ Leuven, Leuven, Belgium.

Received: 13 January 2021 Accepted: 15 June 2021

Published online: 24 June 2021

**References**

- Belver L, Ferrando A. The genetics and mechanisms of T cell acute lymphoblastic leukaemia. *Nat Rev Cancer*. 2016;16(8):494–507.
- Roberts KG. Genetics and prognosis of ALL in children vs adults. *Hematol (United States)*. 2018;2018(1):137–45.
- Ma X, Edmonson M, Yergeau D, et al. Rise and fall of subclones from diagnosis to relapse in pediatric B-acute lymphoblastic leukaemia. *Nat Commun*. 2015;6:1–12.
- De Keersmaecker K, Atak ZK, Li N, et al. Exome sequencing identifies mutation in CNOT3 and ribosomal genes RPL5 and RPL10 in T-cell acute lymphoblastic leukemia. *Nat Genet*. 2013;45(2):186–90.
- De Keersmaecker K, Rocnik JL, Bernard R, et al. Kinase activation and transformation by NUP214-ABL1 is dependent on the context of the nuclear pore. *Mol Cell*. 2008;31(1):134–42.
- Hagemeijer A, Graux C. ABL1 rearrangements in T-cell acute lymphoblastic leukemia. *Genes Chromosomes Cancer*. 2010;49:299–308.
- Vicente C, Schwab C, Broux M, et al. Targeted sequencing identifies associations between IL7R-JAK mutations and epigenetic modulators in T-cell acute lymphoblastic leukemia. *Haematologica*. 2015;100(10):1301–10.
- Liu Y, Easton J, Shao Y, et al. The genomic landscape of pediatric and young adult T-lineage acute lymphoblastic leukemia. *Nat Genet*. 2017;49(8):1211–8.
- Weng AP, Lee W, Sanchez-Irizarry C, et al. Activating mutations of NOTCH1 in human T cell acute lymphoblastic leukemia. *Science*. 2004;306(5694):269–71.
- De Keersmaecker K, Lahortiga I, Mentens N, et al. In vitro validation of gamma-secretase inhibitors alone or in combination with other anti-cancer drugs for the treatment of T-cell acute lymphoblastic leukemia. *Haematologica*. 2008;93(4):533–42.
- Papayannidis C, DeAngelo DJ, Stock W, et al. A Phase 1 study of the novel gamma-secretase inhibitor PF-03084014 in patients with T-cell acute lymphoblastic leukemia and T-cell lymphoblastic lymphoma. *Blood Cancer J*. 2015;5(9):e350–e350.
- Deangelo DJ, Stone RM, Silverman LB, et al. A phase I clinical trial of the notch inhibitor MK-0752 in patients with T-cell acute lymphoblastic leukemia/lymphoma (T-ALL) and other leukemias. *J Clin Oncol*. 2006;24(18\_Suppl):6585–6585.
- Habets RA, de Bock CE, Serneels L, et al. Safe targeting of T cell acute lymphoblastic leukemia by pathology-specific NOTCH inhibition. *Sci Transl Med*. 2019;11(494):6246.
- Borgegård T, Gustavsson S, Nilsson C, et al. Alzheimer's disease: presenilin 2-sparing  $\gamma$ -secretase inhibition is a tolerable  $A\beta$  peptide-lowering strategy. *J Neurosci*. 2012;32(48):17297–305.
- Sanchez-Martin M, Ambesi-Impombato A, Qin Y, et al. Synergistic anti-leukemic therapies in NOTCH1-induced T-ALL. *Proc Natl Acad Sci U S A*. 2017;114(8):2006–11.
- Jabbour E, Kantarjian H. Chronic myeloid leukemia: 2020 update on diagnosis, therapy and monitoring. *Am J Hematol*. 2020;95(6):691–709.
- Vainchenker W, Constantinescu SN. JAK/STAT signaling in hematological malignancies. *Oncogene*. 2012;32:2601–13.
- Braun TP, Eide CA, Druker BJ. Response and resistance to BCR-ABL1-targeted therapies. *Cancer Cell*. 2020;37(4):530–42.
- Vercruyse T, De Bie J, Neggers JE, et al. The second-generation exportin-1 inhibitor KPT-8602 demonstrates potent activity against acute lymphoblastic leukemia. *Clin Cancer Res*. 2017;23(10):2528–41.
- Verbeke D, Demeyer S, Prieto C, et al. The XPO1 inhibitor KPT-8602 synergizes with dexamethasone in acute lymphoblastic leukemia. *Clin Cancer Res*. 2020;26(21):5747–58.
- Etchin J, Berezovskaya A, Conway AS, et al. KPT-8602, a second-generation inhibitor of XPO1-mediated nuclear export, is well tolerated and highly active against AML blasts and leukemia-initiating cells. *Leukemia*. 2017;31(1):143–50.
- Best JD, Smith DW, Reilly MA, et al. The novel secretase inhibitor N-[cis-4-[(4-chlorophenyl)sulfonyl]-4-(2,5-difluorophenyl)cyclohexyl]-1,1,1-trifluoromethanesulfonamide (MRK-560) reduces amyloid plaque deposition without evidence of notch-related pathology in the Tg2576 mouse. *J Pharmacol Exp Ther*. 2006;320(2):552–8.
- Samon JB, Castillo-Martin M, Hadler M, et al. Preclinical analysis of the  $\gamma$ -secretase inhibitor PF-03084014 in combination with glucocorticoids in T-cell acute lymphoblastic leukemia. *Mol Cancer Ther*. 2012;11(7):1565–75.
- O'Neil J, Grim J, Strack P, et al. FBW7 mutations in leukemic cells mediate NOTCH pathway activation and resistance to gamma-secretase inhibitors. *J Exp Med*. 2007;204(8):1813–24.
- Palomero T, Sulis ML, Cortina M, et al. Mutational loss of PTEN induces resistance to NOTCH1 inhibition in T-cell leukemia. *Nat Med*. 2007;13(10):1203–10.
- Medyouf H, Gao X, Armstrong F, et al. Acute T-cell leukemias remain dependent on Notch signaling despite PTEN and INK4A/ARF loss. *Blood*. 2010;115(6):1175–84.
- Girardi T, Vicente C, Cools J, De KK. The genetics and molecular biology of T-ALL. *Blood*. 2016;129(9):1113–23.
- Degrype S, De Bock CE, Cox L, et al. JAK3 mutants transform hematopoietic cells through JAK1 activation, causing T-cell acute lymphoblastic leukemia in a mouse model. *Blood*. 2014;125(7):1107–15.
- Govaerts I, Jacobs K, Vandepoel R, Cools J. JAK/STAT pathway mutations in T-ALL, including the STAT5B N642H mutation, are sensitive to JAK1/JAK3 inhibitors. *HemaSphere*. 2019;3(6):313.
- Graux C, Cools J, Melotte C, et al. Fusion of NUP214 to ABL1 on amplified episomes in T-cell acute lymphoblastic leukemia. *Nat Genet*. 2004;36(10):1084–9.
- Chen B, Jiang L, Zhong ML, et al. Identification of fusion genes and characterization of transcriptome features in T-cell acute lymphoblastic leukemia. *Proc Natl Acad Sci U S A*. 2017;115(2):373–8.
- Zweidler-McKay PA, DeAngelo DJ, Douer D, et al. The safety and activity of BMS-906024, a gamma secretase inhibitor (GSI) with anti-notch activity, in patients with relapsed T-cell acute lymphoblastic leukemia (T-ALL): initial results of a phase 1 trial. *Blood*. 2014;124(21):968–968.

**Publisher's Note**

Springer Nature remains neutral with regard to jurisdictional claims in published maps and institutional affiliations.